ELSEVIER

Spectrochimica Acta Part B 59 (2004) 1725–1731

SPECTROCHIMICA ACTA PART B

www.elsevier.com/locate/sab

A library for X-ray–matter interaction cross sections for X-ray fluorescence applications☆

A. Brunetti[a,b,*], M. Sanchez del Rio[c], B. Golosio[b,c], A. Simionovici[c,d], A. Somogyi[c]

[a]*Istituto di Matematica e Fisica, Universita' di Sassari, via Vienna 2, 07100 Sassari, Italy*
[b]*INFN, Sezione di Cagliari, Italy*
[c]*European Synchrotron Radiation Facility, 6 rue Jules Horowitz, 38043 Grenoble Cedex, France*
[d]*Laboratoire de Sciences de la Terre, École Normale Supérieure, Lyon, F-69364*

Received 1 November 2003; accepted 19 March 2004
Available online 2 September 2004

Abstract

Quantitative estimate of elemental composition by spectroscopic and imaging techniques using X-ray fluorescence requires the availability of accurate data of X-ray interaction with matter. Although a wide number of computer codes and data sets are reported in literature, none of them is presented in the form of freely available library functions which can be easily included in software applications for X-ray fluorescence. This work presents a compilation of data sets from different published works and an *xraylib* interface in the form of callable functions. Although the target applications are on X-ray fluorescence, cross sections of interactions like photoionization, coherent scattering and Compton scattering, as well as form factors and anomalous scattering functions, are also available.

Keywords: Library; X-ray; Fluorescence

1. Introduction

Quantitative analysis of X-ray measurements requires the computation of cross sections and atomic parameters. Several databases and tabulations are available in the literature. For example, at the NIST web site it is possible to find a complete set of cross sections separated by type of interaction [1,2]. Another well-known collection of data is the EPDL database from the Lawrence Livermore National Laboratory [3]. It contains a complete set of total and partial cross sections, as well as form factors and scattering functions. The RTAB data by Kissel [4] contains a complete set of elastic photon–atom scattering data.

For the specific case of X-ray fluorescence (XRF) applications, only two published tabulations are found in the literature, the first due to Krause et al. [5] and the second due to Puri et al. [6]. Krause et al. report a complete set of XRF cross sections, as well as useful formulas and all the necessary parameters needed for computing the XRF cross sections, including fluorescence yield, fractional radiation rates, etc. Puri's tabulation, although less exhaustive, claims to update some of the data. Direct comparison between these two tabulations is in general not possible, as the first one tabulates individual lines, and the second one some groups of lines. Puri gives some notes on the comparison of its data with Krause's data: XRF K-line cross sections are in good agreement for atoms with $Z \geq 20$, but they differ by values up to 10% for light elements. Values of XRF L_α cross sections differ by more than 10% over most atomic regions. Puri points out that these discrepancies are mainly due to the differences in the values of the L subshell fluorescence yield and Coster–Kronig (CK) rates.

☆ This paper was presented at the International Congress on X-Ray Optics and Microanalysis (ICXOM XVII), held in Chamonix, Mont Blanc, France, 22-26 September 2003, and is published in the special issue of *Spectrochimica Acta Part B*, dedicated to that conference.

* Corresponding author. Istituto di Matematica e Fisica, Universita' di Sassari, via Vienna 2, 07100 Sassari, Italy. Tel.: +39 79 229483; fax: +39 79 229482.
E-mail address: brunetti@uniss.it (A. Brunetti).

0584-8547/$ - see front matter © 2004 Elsevier B.V. All rights reserved.
doi:10.1016/j.sab.2004.03.014

Table 1
Names, input and output of the *xraylib* functions

Category	Function	Returns
Atomic data	float AtomicWeight(int Z)	atomic weight
Cross sections: (cm^2/g)	float CS_Total(int Z, float E)	Total cross section (photoionization+ Rayleigh+ Compton)
	float CS_Photo(int Z, float E)	Photoionization CS
	float CS_Rayl(int Z, float E)	Rayleigh CS
	float CS_Compt(int Z, float E)	Compton CS
	float CS_FluorLine(int Z, int line, float E)	XRF CS
Cross sections: (barn/atom)	float CS_KN(float E)	Klein-Nishina CS
	float CSb_Total(int Z, float E)	Total cross section (photoionization+ Rayleigh+ Compton)
	float CSb_Photo(int Z, float E)	Photoionization CS
	float CSb_Rayl(int Z, float E)	Rayleigh CS
	float CSb_Compt(int Z, float E)	Compton CS
	float CSb_FluorLine(int Z, int line, float E)	XRF CS
Differential unpolarized cross sections: ($cm^2/g/sterad$)	float DCS_Rayl(int Z, float E, float theta)	Rayleigh DCS
	float DCS_Compt(int Z, float E, float theta)	Compton DCS
Differential unpolarized cross sections: (barns/atom/ sterad)	float DCS_Thoms(float theta)	Thomson DCS
	float DCS_KN(float E, float theta)	Klein–Nishina DCS
	float DCSb_Rayl(int Z, float E, float theta)	Rayleigh DCS
	float DCSb_Compt(int Z, float E, float theta)	Compton DCS
Form factors, scattering functions, momentum transfer	float FF_Rayl(int Z, float q)	Rayleigh
	float SF_Compt(int Z, float q)	Incoherent scattering function
	float MomentTransf(float E, float theta)	Momentum transfer (A^-1)
Compton energy	float ComptonEnergy(float E0, float theta)	Photon energy after Compton scattering
Absorption edges and transitions data	float EdgeEnergy(int Z, int shell)	Absorption edge energy [keV]
	float LineEnergy(int Z, int line)	Fluorescence line energy [keV]
	float FluorYield(int Z, int shell)	Fluorescence yield
	float JumpFactor(int Z, int shell)	Jump ratio
	float RadRate(int Z, int line)	Radiation rate
	float CosKronTransProb(int Z, int trans)	Coster–Kronig transition probability

It is possible to directly use the data from these tabulations for software applications. Both data sets come in a paper format, but it is possible to transcribe the data into electronic format. However, this is a very rigid approach, because it is not possible to verify and upgrade the data contributing to the fluorescence cross section, to get accurate interpolated data (as the energy step for the tabulations is usually quite large), and use fluorescence lines other than the tabulated. Moreover, these references are quite old and although there is no new published compilation of XRF cross sections, there was in the last years remarkable progress in evaluated data, in particular for photoionization cross section and anomalous scattering factors [2–4,7], and fluorescence yields [8]. It is therefore interesting to benefit from these new and more accurate data for the calculations of the XRF cross section. Thus, our approach is to evaluate XRF from its components, and not using published tables of XRF cross sections.

An attempt to solve the problem of interfacing the data to the user is reported by Elam et al. [9]. They used a selection of previously published data. Although we found this tabulation extremely useful, we found difficulties in using it for XRF purposes. We present here a new database, which is loaded by a software package based on a shared C language library. Our interface functions are easily imported into languages used in scientific programming like C, Fortran and Python, and run in most operating systems. XRF data produced by our library are compared Krause data [5] and the differences are discussed. This library has been shown to be a valuable tool for several applications we developed that require a quick access to data, like fast spectroscopy reconstructions and Monte Carlo simulations.

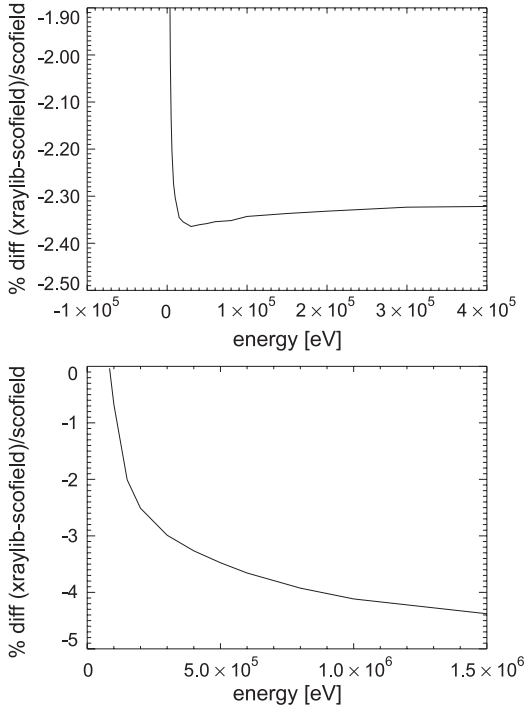

Fig. 1. Relative differences between the XRF cross sections (or partial photoionization cross section) using the full partial cross section tabulation (Scofield) and the jump approximation (in *xraylib*), for Z=13 (top) and Z=80 (bottom).

2. The *xraylib* function interface

In quantitative analysis of X-ray fluorescence, one needs to access different X-ray data in a quick way. For example, when analysing an XRF spectrum, the different lines corresponding to the trace elements can be analysed separately. In first approximation (thick target, primary fluorescence), the X-ray intensity at the detector can be written as [10]

$$I_{\mathrm{el}} = I_{\mathrm{o}} \frac{\Omega}{4\pi} \frac{\sigma_{\mathrm{XRF}}(E_0)}{\sigma_{\mathrm{TOT}}(E_0)} \frac{1}{\sin\psi_1} \frac{C_{\mathrm{el}} \propto_{\mathrm{el}}(E_0)}{\frac{\propto(E_0)}{\sin\psi_1} + \frac{\propto(E_1)}{\sin\psi_2}} \tag{1}$$

where I_1 is the XRF intensity for a trace element "el" of weight concentration C_{el}, I_0 is the incident photon intensity at energy E_0, Ω is the detector solid angle, σ_{XRF} and σ_{PE} are the fluorescence and photoionization cross sections, respectively, ψ_1 (ψ_2) is the incident (take off) angle measured with respect to the sample surface, and $\propto_{\mathrm{el}}$ and $\propto$ are the attenuation coefficients of the trace element and matrix, respectively.

In order to evaluate this equation, it is necessary to calculate different cross sections and attenuation coefficients for the matrix and trace element considered at two energies, the incident photon energy and the energy of the considered line. In *xraylib*, we provide functions that can calculate each of these ingredients in a single line of code. The names of the functions are in Table 1.

The function interface, written in ANSI C, can be linked with any program written in C, C+ or Fortran. Moreover, the *xraylib* library can be bound to software in different programming languages, provided that a C linking is available. The *xraylib* library has been tested in Macintosh OSX, Linux and Microsoft Windows operating systems. It has also been bound to the two high-level shell languages IDL and Python. It is also possible to access the database just as a "pocket calculator", i.e., by using a set of command line instructions, developed in a Python shell script.

3. XRF cross-section calculations

For the calculation of the XRF cross sections, the following formulas are used [5]

$$\sigma_{K\alpha_{K\beta}} = \sigma_K(E)\omega_K F_{K\alpha_{K\beta}} \tag{2}$$

$$\sigma_{\mathrm{L}_1 j} = \sigma_{\mathrm{L}_1}\omega_1 F_{\mathrm{L}_1 j} \tag{3}$$

where σ_{k} is the K-shell cross section; ω_{k} is the K-shell fluorescence yield; F is the fractional emission rate ($F_{\mathrm{k}\alpha,\beta}=I_{\mathrm{k}\alpha}+I_{\mathrm{k}}\beta$); j are the transitions ending in L_1. Krause gives values for the transitions $\mathrm{L}_1\mathrm{L}_{23}$, $\mathrm{L}_1\mathrm{M}_3$ ($\mathrm{L}\beta_3$) and $\mathrm{L}_1\mathrm{O}_{23}$ ($\mathrm{L}\gamma_4$),

$$\sigma_{L_2 j} = \sigma_{L_2}\omega_2 F_{L_2 j} + \sigma_{L_1}\omega_2 F_{L_2 j} f_{1,2} \tag{4}$$

where now j are the transitions ending in L_2 and the f are the Coster–Kronig yields. In Krause there are: $\mathrm{L}_2\mathrm{M}_4$ ($\mathrm{L}\beta_1$) and $\mathrm{L}_2\mathrm{N}_4$ ($\mathrm{L}\gamma_1$), and

$$\sigma_{\mathrm{L}_3 j} = \sigma_{\mathrm{L}_3}\omega_3 F_{\mathrm{L}_3 j} + \sigma_{\mathrm{L}_2}\omega_3 F_{\mathrm{L}_3 j} f_{2,3} + \sigma_{\mathrm{L}_1}\omega_3 F_{\mathrm{L}_3 j}\left(f_{1,3} + f_{1,3}' + f_{1,2} f_{2,3}\right) \tag{5}$$

here j are the transitions ending in L_3: for $\mathrm{L}_3\mathrm{M}_5$ ($\mathrm{L}\alpha_1$), $\mathrm{L}_3\mathrm{N}_{45}$ ($\mathrm{L}\beta_{2,15}$), $\mathrm{L}_3\mathrm{M}_1$ (Ll)

These expressions need the partial (for K, L_1, L_2 and L_3) photoionization cross sections as a function of the photon energy. Commonly used tabulations are those of Scofield [11], EPDL [3] and Kissel [4]. As the storage and access of these data is cumbersome, it is in many cases useful to store the so-called "jumping ratio", or the ratio between the photoionization cross section after the edge (typically 1 eV after the edge) divided by the value before the edge. For example, for the K-edge:

$$J_{\mathrm{K}}(E) = \frac{\sigma_{\mathrm{after}}}{\sigma_{\mathrm{before}}} = \frac{\sigma_{\mathrm{T}}}{\sigma_{\mathrm{T}} - \sigma_{\mathrm{K}}} \tag{6}$$

This jumping ratio, by definition, depends only on the atomic element and shell, and it is not a function of the energy; therefore, its storage and access is lighter. We can write the partial cross sections approximately as:

$$\sigma_{\mathrm{K}}(E) = \sigma_{\mathrm{PE}}(E)\tau_0; \quad \sigma_{\mathrm{L}_{(3,2,1)}}(E) = \sigma_{\mathrm{PE}}(E)\tau_{(3,2,1)} \tag{7}$$

and the τ values taken are

$$\tau_0 = \frac{J_{\mathrm{K}} - 1}{J_{\mathrm{K}}} \tag{8}$$

and

	$E<E_{\mathrm{L3}}$	$E_{\mathrm{L3}}<E<E_{\mathrm{L2}}$	$E_{\mathrm{L2}}<E<E_{\mathrm{L1}}$	$E_{\mathrm{L1}}<E<E_{\mathrm{K}}$	$E_{\mathrm{K}}<E$
τ_1	0	0	0	$(J_{\mathrm{L1}}-1)/J_{\mathrm{L1}}$	$(J_{\mathrm{L1}}-1)/(J_{\mathrm{K}}J_{\mathrm{L1}})$
τ_2	0	0	$(J_{\mathrm{L2}}-1)/J_{\mathrm{L2}}$	$(J_{\mathrm{L2}}-1)/(J_{\mathrm{L1}}J_{\mathrm{L2}})$	$(J_{\mathrm{L2}}-1)/(J_{\mathrm{K}}J_{\mathrm{L1}}J_{\mathrm{L2}})$
τ_3	0	$(J_{\mathrm{L3}}-1)/J_{\mathrm{L3}}$	$(J_{\mathrm{L3}}-1)/(J_{\mathrm{L2}}J_{\mathrm{L3}})$	$(J_{\mathrm{L3}}-1)/(J_{\mathrm{L1}}J_{\mathrm{L2}}J_{\mathrm{L3}})$	$(J_{\mathrm{L3}}-1)/(J_{\mathrm{K}}J_{\mathrm{L1}}J_{\mathrm{L2}}J_{\mathrm{L3}})$

It is clear that use of jump ratios gives correct result only in the case that the incident photons have energies slightly higher than the edge of the selected element. This is not the case of standard XRF, where the energy of the incident photons is set several kiloelectron volts higher than the energy if the highest line. We have calculated the differences of the XRF cross sections using the jump approximation (*xraylib* version 2.3) and the Scofield's partial cross sections (Fig. 1). We see errors of few percent due to this approximation for the K lines. For the L lines the differences are much more important. In Table 2 we can see the example of Ca. At energies where τ_i depends only on J_{Li}, we have errors of the order of 50% for L_3 lines, 20% for L_2 and more than 400% for L_1. After many numerical comparisons with Krause tabulations, we concluded that the jump approximation can be safety used for K lines, should be used with care for L_3 and L_2, and should never be used for L_1 lines. XRF cross sections given by *xraylib* 2.3 (using the jump approximation) are compared with Krause data in the "*xraylib* tables", an electronic document available with the *xraylib* distribution. As a result of this study, we decided to implement the full partial cross sections that will be available in next version of *xraylib*.

Important discrepancies in calculated XRF cross sections are found depending on the used values of fluorescence yield and fractional radiative rates. As there is a linear dependence of the XRF on these parameters, they are discussed in the next section. Plots of the XRF fluorescence cross sections calculated by *xraylib* are shown in Fig. 2.

4. The *xraylib* database: cross sections and other X-ray functions

The *xraylib* functions are the user interface for internally stored data. These data files are not supposed to be modified or accessed by the user. However, we have chosen to use only ASCI data files in order to be easily human-readable and to be able, if necessary, to access and modify them.

Table 2
Input and output variable description

Meaning	Name	Values/Unit
Atomic number	Z	1–100
Energy	E	keV
Scattering polar angle	theta	rad
Scattering azimuthal angle	phi	rad
Momentum transfer	q	
Atomic electron shell	shell	K_SHELL 0
		L1_SHELL 1
		L2_SHELL 2
		L3_SHELL 3
		M1_SHELL 4
		M2_SHELL 5
		M3_SHELL 6
		M4_SHELL 7
		M5_SHELL 8
Fluorescence Line	line	KA_LINE 0 ($K\alpha_1$+$K\alpha_2$)
		KB_LINE 1 ($K\beta_1$+$K\beta_3$)
		KL3_LINE −3 ($K\alpha_1$)
		KL2_LINE −2 ($K\alpha_2$)
		KM3_LINE −6 ($K\beta_1$)
		KM2_LINE −5 ($K\beta_3$)
		LA_LINE 2
		($L\alpha_1$)(or L3M5_LINE −42)
		LB_LINE 3
		($L\beta_1$)(or L2M4_LINE −29)
		L3M1_LINE −38 (L*l*)
		L2N4_LINE −34 ($L\gamma_1$)
		L1M3_LINE −16 ($L\beta_3$)
CK transition probability	trans	F1_TRANS 0
		F12_TRANS 1
		F13_TRANS 2
		FP13_TRANS 3
		F23_TRANS 4

Only the lines of which XRF cross section can be calculated with *xraylib* are displayed.

4.1. Cross section data (Compton, Rayleigh and photoionization)

Data sets of cross sections of different mechanisms of interaction atom–photons are given: Compton, Rayleigh and photoionization. In the current version (*xraylib* 2.3), these tabulations are those of Elam et al. [9 and references therein]. In order to obtain numerical values of cross sections for an arbitrary energy, a cubic spline interpolation of the logarithm of the cross section versus the logarithm of the energy [12] has been implemented. This approach is the one also used in Ref. [13]. However, the type of implementation of the cubic spline is different. In our case, we used the routine for cubic spline interpolation from Ref. [12], the same routine used by Elam et al. This routine comes as a set of three values for each energy, where the third value is the second derivative value. The latter value allows one to control the behaviour of the interpolation at the edges where a second derivative value of zero is used. In this way, the sharp transitions at absorption edges can be managed and only one tabulation can be used. The photoionization cross sections given by Elam et al. contain, for energy higher than 1 keV, the cross sections tabulated by Hubbell [13] and for energy lower than 1 keV the tables from Plechaty et al. [14]. The cross section values at the absorption edges are given by two values, one just below the edge and the other just above the edge, both having the same energy value but not giving any problems with the interpolation.

The CS_FluorLine function allows calculating the XRF cross sections, and this function makes use of the partial photoionization cross sections (calculated via the jumping ratio, as previously described), fluorescence yields and fractional emission rates of the lines considered. It is also possible to obtain an averaged photoionization cross section for the K lines, avoiding the division in sub lines. This is

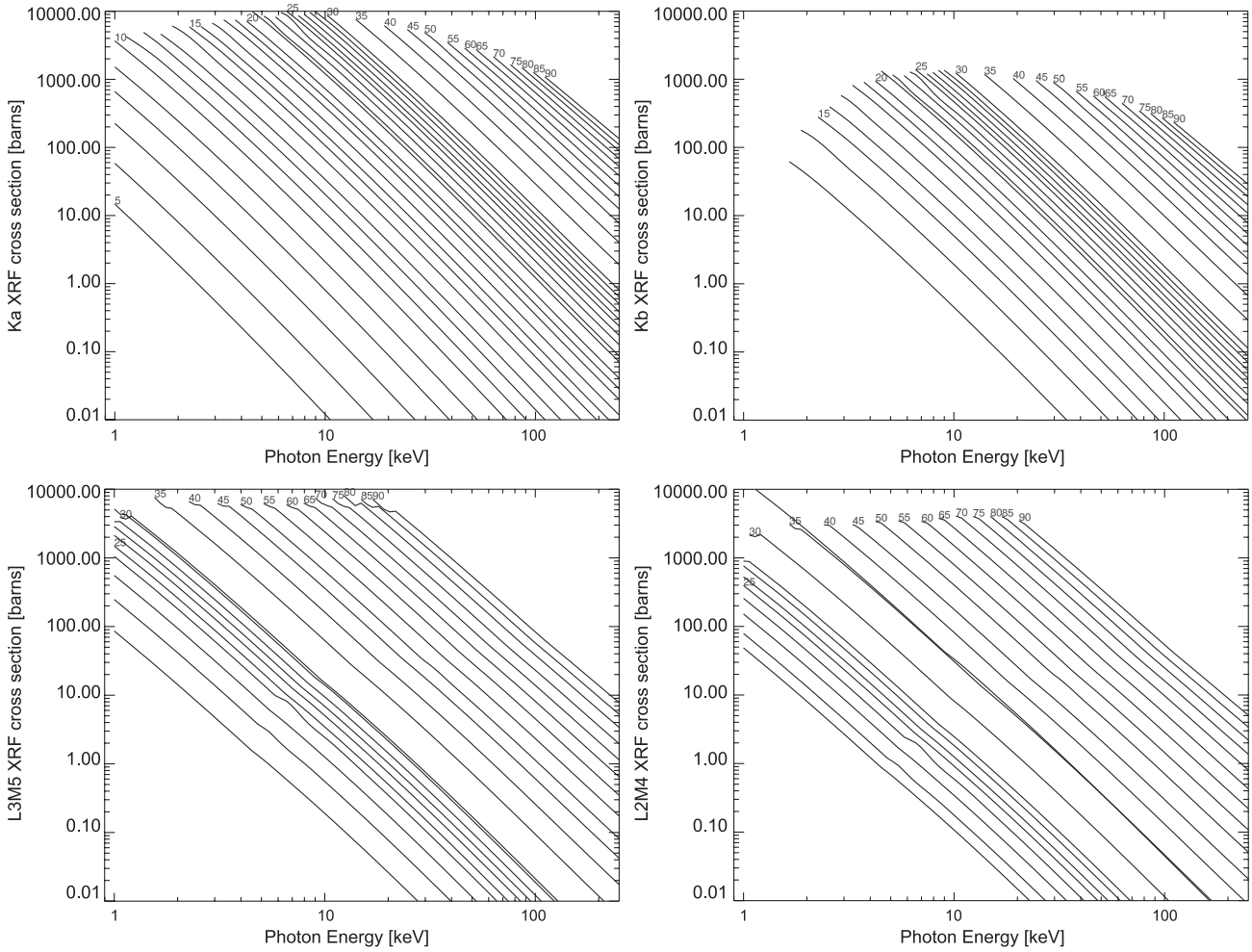

Fig. 2. Plots of the XRF cross sections for Kα (KL3+KL2) (top left), Kβ (KM2+KM3) (top right), $L\alpha_1$ (L3M3) (bottom left) and $L\beta_1$ (L2M4) (bottom right). The parameter on the curves is the atomic number.

useful in the case when the detector used cannot resolve all the lines of the individual transitions finishing in a given shell.

We are currently changing the photoionization tabulations in order to include partial shell cross sections. These data are available in Scofield's and Kissel's data sets as well as the EPDL database. The use of partial cross sections improves the values of the XRF cross sections by 2–10% for the K lines, as discussed before, and is even more important for the L lines.

4.2. Jump ratio, fluorescence yield, Coster–Kronig transition probabilities, relative radiative rates

Jump ratios are those tabulated by Elam et al. [9]. Coster–Kronig and radiative rates are taken from Krause et al. [5]. Fluorescence yields are from Table 4 of Hubbell et al. [8]. As XRF cross sections depend linearly on the fluorescence yields and on the radiative rates, the errors in these values propagate directly to the XRF cross sections.

Let us take, for example, the K-shell fluorescence yield of Al (Z=11): Hubbell et al. [8] in Table 3 give 0.033 as an "averaged" value (used in *xraylib*). However, Krause's [15,5] value is 0.039 and his "condensed matter" value is 0.036. The value chosen by Elam et al. [9] is 0.033. These differences, affecting the XRF cross sections, may be as high as 20%.

It is then desirable to use the most accurate values available, although the choice is not simple.

4.3. Differential scattering cross sections

The differential cross sections calculated by *xraylib* use the following equations.

Differential Thomson cross section:

$$\frac{d\sigma_T(\theta)}{d\Omega} = \frac{r_e^2}{2}\left(1+\cos^2\theta\right) \tag{9}$$

where θ is the scattering angle and r_e is the classical radius of the electron.

Table 3
Values of τ calculated using the jump approximation and Scofield [11] data (made available by Kissel [4]) for Ca (Z=20)

Edge	Energy [keV]	τ_x (*xraylib*)	τ_s (Scofield)	τ_s/τ_x
K	14.701	0.886	0.906	1.024
K	36.025	0.886	0.909	1.027
K	57.350	0.886	0.910	1.028
K	78.675	0.886	0.910	1.028
K	100.000	0.886	0.910	1.028
L1	0.838	0.105	0.223	2.128
L1	1.638	0.105	0.313	2.991
L1	2.438	0.105	0.380	3.630
L1	3.238	0.105	0.455	4.347
L1	4.038	0.105	0.068	0.648
L2	0.360	0.286	0.234	0.819
L2	0.379	0.286	0.234	0.818
L2	0.399	0.286	0.234	0.818
L2	0.418	0.286	0.234	0.818
L2	0.438	0.286	0.233	0.817
L3	0.347	0.828	0.458	0.553
L3	0.347	0.828	0.458	0.553
L3	0.348	0.828	0.458	0.553
L3	0.349	0.828	0.458	0.553
L3	0.350	0.828	0.458	0.553
L3	0.350	0.828	0.458	0.553

Differential Klein–Nishina cross section:

$$\frac{d\sigma_{K-N}(\theta,E)}{d\Omega} = \frac{r_e^2}{2}\left(\frac{K}{K_0}\right)^2\left(\frac{K}{K_0}+\frac{K_0}{K}-\sin^2\theta\right) \quad (10)$$

where

$$\frac{K_0}{K} = 1+\frac{E_i}{m_e c^2}(1-\cos\theta) \quad (11)$$

Differential Rayleigh cross section:

$$\frac{d\sigma_R(\theta)}{d\Omega} = \frac{d\sigma_T(\theta)}{d\Omega}F^2(x,Z) = \frac{r_e^2}{2}\left(1+\cos^2\theta\right)F(x,Z) \quad (12)$$

Differential Compton cross section:

$$\frac{d\sigma_C(\theta,E)}{d\Omega} = \frac{d\sigma_{K-N}(\theta,E)}{d\Omega}S(x,Z) = \frac{r_e^2}{2}\left(\frac{K}{K_0}\right)^2\left(\frac{K}{K_0}+\frac{K_0}{K}-\sin^2\theta\right)S(x,Z) \quad (13)$$

It also possible to evaluate the polarization-dependent values of these cross sections.

4.4. Form factor and scattering function

The form factor and scattering function come from the Hubbell [13] and Cullen et al. [3] compilations. The forms factors are the non-relativistic data calculated by Hubbell. He also calculated the relativistic and relativistic modified form factors. However, he recommended to use the non-relativistic data because they are closer to the experimental data. The anomalous scattering functions are due to Cullen et al. [3] who evaluated them from photoionization cross sections using the relativistic dispersion relation.

4.5. Atomic parameters

The edge energies are from the tabulation by Larskin [16] reported in Ref. [17]. The energies of the fluorescence lines are the experimental values of Deslattes et al. [18]. Whenever the experimental value is missing, the theoretical one from the same reference is used. Moreover, we used for the $K_{\alpha 1}$ for Z=3–9, absent in the reference, the values from Ref. [19].

5. Conclusions and perspectives

A new database, with a user interface in the form of a C callable library, has been developed for XRF and other X-ray applications. The library has been tested for the last 6 months at both the ESRF and at the Institute of Mathematics and Physics of the University of Sassari for Monte Carlo simulations and other on-line applications. It is freely available at http://ftp.esrf.fr/pub/scisoft/xraylib. From this site, in addition to the library, database and source code, a printable file with XRF cross sections and other data can be downloaded. The library is continuously updated and the user is referred to the documentation therein. We would also like to continue the tests against experimental data, in order to improve the quality of the tables. Future developments will be in the direction of introducing new functionalities, such as the double differential Compton cross section, which is an essential option for Monte Carlo simulations.

Acknowledgments

This work was performed partly under the auspices of the NATO Scientific Affairs Division, through grant no. EST-CLG-979530.

References

[1] J.H. Hubbell, J.S. Coursey, J. Hwang, D.S. Zucker, Bibliography of Photon Total Cross Section (Attenuation Coefficient) Measurements (version 2.2), National Institute of Standards and Technology, Gaithersburg, MD, 1998, [Online]. Available: http://physics.nist.gov/photoncs [2003, June 4].
[2] M.J. Berger, J.H. Hubbell, S.M. Seltzer, J.S. Coursey, D.S. Zucker, XCOM: Photon Cross Section Database (version 1.2), National Institute of Standards and Technology, Gaithersburg, MD, 1999, [Online] Available: http://physics.nist.gov/xcom [2003, November 6].
[3] D.E. Cullen, J.H. Hubbell, and L. Kissel, Lawrence Livermore National Laboratory Report, UCRL-50400, 6 rev 5 (1997).
[4] L. Kissel, Radiat. Phys. Chem. 59 (2000) 185–200 (http://www-phys.llnl.gov/Research/scattering/RTAB.html).
[5] M.O. Krause, C.W. Nestor Jr., C.J. Sparks Jr., E. Ricci, X-ray fluorescence cross sections for K and L X-rays of the elements ORNL-5399 (Oak-Ridge) (1978).
[6] S. Puri, B. Chand, D. Mehta, M.L. Garg, N. Singh, P.N. Trehan, At. Data Nucl. Data Tables 61 (1995) 289–311.
[7] C.T. Chantler, K. Olsen, R.A. Dragoset, A.R. Kishore, S.A. Kotochigova, D.S. Zucker, X-ray form factor, attenuation and scattering tables (version 2.0), 2003 [Online] Available: http://

physics.nist.gov/ffast [2003, November 7]; National Institute of Standards and Technology, Gaithersburg, MD. Originally published as C.T. Chantler, J. Phys. Chem. Ref. Data 29(4), 597–1048 (2000); C.T. Chantler, J. Phys. Chem. Ref. Data 24 (1995) 71–643.
[8] J.H. Hubbell, et al., A review, bibliography and tabulation of K, L and higher atomic shell X-ray fluorescence yields, J. Phys. Chem. Ref. Data 23 (1994) 339–364.
[9] W.T. Elam, B.D. Ravel, J.R. Sieber, Radiat. Phys. Chem. 63 (2002) 121.
[10] G.R. Lachance, F. Claisse, Quantitative X-ray fluorescence analysis, Theory and Applications, John Wiley, 1995.
[11] J.H. Scofield,“ Theoretical Photoionization Cross Sections from 1 to 1500 keV”, Lawrence Livermore Laboratory Report UCRL-51326, Livermore, Ca (1973).
[12] W.H. Press, S.A. Teukolsky, W.T. Vetterling, B.P. Flannery, Numerical Recipes in Fortran. The Art of Scientific Computing, 2nd edition, Cambridge University Press, 1992.
[13] J.H. Hubbel, et al., Atomic form factors, incoherent scattering functions and photon scattering cross sections, J. Phys. Chem. Ref. Data 4 (1975) 471.
[14] E.F. Plechaty, D.E. Cullen, R.J. Howerton, Tables and graphs of photon interaction cross sections from 0.1 keV to 100 MeV derived from LLL evaluated nuclear data library. Lawrence Livermore National Laboratory Report, UCRL-50400, 6, rev 3. (1981).
[15] M.O. Krause, J. Phys. Chem. Ref. Data 8 (1979) 307.
[16] F.B. Larkins, At. Data Nucl. Data Tables 20 (1977) 313.
[17] Table of Isotopes CD-ROM Eighth Edition, Version 1.0, March 1996. Richard B. Firestone Virginia S. Shirley, Editor Coral M. Baglin and Jean Zipkin Lawrence Berkeley National Laboratory, University of California S.Y. Frank Chu, CD-ROM Editor, Wiley-Interscience.
[18] R.D. Deslattes, E.G. Kessler Jr., P. Indelicato, L. de Billy, E. Lindroth, J. Anton, Rev. Mod. Phys. 75 (2003) 35–99.
[19] J.A. Bearden, Rev. Mod. Phys. 39 (1967) 78.